Available online at www.sciencedirect.com
ScienceDirect
Ceramics International 36 (2010) 2281–2286
CERAMICS INTERNATIONAL
www.elsevier.com/locate/ceramint

Effect of sintering temperature on the microstructure and mechanical properties of ZrO_2-3 mol%Y_2O_3 sol–gel films

A. Díaz-Parralejo [a,*], A.L. Ortiz [a], R. Caruso [b]

[a] Dpto. de Ingeniería Mecánica, Energética y de los Materiales, Escuela de Ingenierías Industriales, Univ. de Extremadura, Avda. de Elvas, s/n, 06071 Badajoz, Spain
[b] Instituto de Física Rosario (CONICET-UNR), Avda. 27 de Febrero, 210 Bis, 2000 Rosario, Argentina

Received 14 April 2010; received in revised form 27 April 2010; accepted 2 June 2010
Available online 4 August 2010

Abstract

The microstructural evolution and mechanical properties of ZrO_2-3 mol%Y_2O_3 films were investigated as a function of the sintering temperature in the range from 100 °C to 1500 °C, using a battery of characterization techniques including X-ray diffraction (XRD), scanning electron microscopy (SEM), atomic force microscopy (AFM) and nanoindentation. It was found that the crystallization occurs at temperatures close to 300 °C. A gradual increase in the grain and crystallite sizes is observed as the sintering temperature increases up to 1000 °C, and above this sintering temperature the tendency changes abruptly with a rapid increase in these values. Although Young's modulus of the coatings did not change with sintering temperature, a slight decrease was observed in the hardness values above 1000 °C which is attributed to microstructure coarsening. Finally, a slight degradation of the films occurs above 1300 °C, which is due to the occurrence of a process of grain spheroidization.

Keywords: Mechanical properties; ZrO_2; Ceramic films; Microstructure

1. Introduction

The sol–gel method is widely used for the preparation of inorganic materials from solutions containing metals, and is usually referred to as a wet chemical method of producing ceramic materials [1,2]. It is used by a growing number of researchers for the preparation of an extensive variety of new materials, in the form of bulks, membranes, fibres and very especially for the preparation of thin films. There are different techniques to obtain thin films (physical vapour deposition, chemical vapour deposition, sputtering, dip-coating, etc.) [3]. Coating is an important application of the sol–gel process because it presents certain advantages over other techniques: simple equipment and low cost, possibility of coating large areas, high optical quality of films, etc. In addition, it is suitable to obtain almost any single or multi-component oxide coating (ZrO_2, SiO_2, TiO_2, etc.).

In particular, sol–gel zirconia (ZrO_2) coatings have technological importance for applications as protection barriers due to their interesting chemical and mechanical properties [4]. Indeed, zirconia has a large thermal expansion coefficient ($10 \times 10^{-6}\ °C^{-1}$) which is of the same order as those of metallic substrates (from 10 to $20 \times 10^{-6}\ °C^{-1}$), and its thermal conductivity (0.05 cal $cm^{-1}\ °C^{-1}\ s^{-1}$) is one order of magnitude less than those of metals, enabling it to be used as an effective thermal barrier coating. Also, yttria (Y_2O_3) doped zirconia can exhibit good mechanical properties, combining high wear resistance with moderate toughness, frequently associated with the activation of a transformation toughening mechanism [5]. In addition, zirconia has a high refractive index (2.21 at a wavelength of $\lambda = 630$ nm), low absorption, and large optical band gap (3.8–3.2 eV), and therefore its corresponding films have proven very useful for many optical applications.

The structure and properties of thin films can differ significantly from those of the bulk material. In particular, thin film properties depend on porosity, microstructure, and especially on thickness rendering control of characteristics during the densification and sintering processes a critical issue in thin film preparation [6,7]. Consequently, various studies have been conducted to investigate the microstructure and mechanical properties of zirconia sol–gel thin films in order to optimize their behaviour under working conditions [8,9].

* Corresponding author.
E-mail address: adp@unex.es (A. Díaz-Parralejo).

0272-8842/$36.00
doi:10.1016/j.ceramint.2010.07.033

However, the existing studies have mainly focused either on concrete synthesis and processing conditions or on a relatively narrow sintering temperature range.

In the present work the microstructural evolution and mechanical properties of ZrO_2-3 mol%Y_2O_3 (3YSZ) dip-coatings on sapphire substrates has been investigated as a function of sintering temperature up to 1500 °C, a range that have been scarcely studied although it is of particular interest since at these high temperatures the coatings may suffer a severe tear. In particular, we have investigated by X-ray diffraction (XRD) the crystallization process and the phases present in the 3YSZ films. We have also studied the microstructural evolution in the films using XRD, scanning electron microscopy (SEM) and atomic force microscopy (AFM). Finally, we have carried out a mechanical characterization of the 3YSZ films using nanoindentation to determine their hardness (H) and Young's modulus (E) [10–12].

2. Experimental method

2.1. Preparation of solutions and coatings

The starting solution was prepared by mixing and stirring zirconium (IV) n-propoxide 70 wt% diluted in 2-propanol (ZNP) with propanol (PrOH) and with nitric acid (HNO_3) as catalyst in an anhydrous nitrogen atmosphere to avoid hydroxide precipitation [13]. To prepare precursor solutions for 3YSZ films, the starting solution was mixed with a second solution of yttrium (III) acetate ($YAc{\cdot}4H_2O$) dissolved in PrOH and HNO_3. After 1 h, distilled water was added with continuous stirring of the mixture for an additional 10 h, to finally obtain a very homogeneous solution. The $ZNP/PrOH/H_2O/HNO_3$ molar ratios of the final solution were 1/15/5/1. The density, viscosity, oxide concentration and pH of the solution were 0.895 g cm^{-3}, 5.1×10^{-3} Pa s, 78 g L^{-1} and 0.5, respectively.

Sapphire 2.5 × 7.6 cm sheets (supplied by Goodfellow Ltd.) were used as substrates. This selection allows the films to be sintered up to temperatures $T \leq 1500$ °C without substrate degradation. The substrates were previously immersed in acetic acid for 24 h, then cleansed in distilled water and finally in ethanol in an ultrasonic bath for 15 min. Soda-lime glasses have been used as the substrates but only for determining the crystallization temperature.

Preparation of 3YSZ films was performed using the dip-coating method [14]. The withdrawal rate corresponding to each deposit step was suitably selected to obtain crack-free films [7]. The films were deposited on the substrate under an air atmosphere and then dried for 2 h at 100 °C [15]. The dry films were sintered in air at temperatures in the range of 100 °C $\leq T \leq$ 1500 °C for 2 h. The dipping process and sintering treatment were repeated to obtain coatings (2–10 layers) with a total thickness of about 2 μm, in order to avoid the influence of the substrate when measuring the mechanical properties of the 3YSZ films.

2.2. Characterization of the coatings

X-ray diffractometry (XRD) was used for the phase identification and microstructural analyses of the 3YSZ films. The XRD patterns were obtained using a Philips PW-1800 diffractometer with Cu Kα radiation (λ = 1.54183 Å) and a secondary graphite monochromator. The generator settings were 40 kV and 35 mA. The diffraction data were collected over a 2θ range of 20–90° with a step width of 0.05° and a counting time of 5 s per step. Subsequently, XRD patterns were analyzed using the Rietveld program BGMN [16].

A Park Scientific Instrument atomic force microscope (AFM) was used in contact mode to obtain quantitative surface topographical images of the coatings. Microfabricated Si_3N_4 integrated pyramidal tips were used in scanning. The cantilevers had a force constant of 0.4 N/m and radius of curvature of 100 Å.

A scanning electron microscope (SEM) was used to study details of the microstructural evolution in the 3YSZ films. The SEM samples were previously gold sputtered to avoid phenomena of accumulation of local charge on the surface of the sample. The observations were made in a SEM Hitachi S-3600N, operating under a voltage of 20 kV and an emission current of 68 mA.

Nanoindentation tests were conducted to study the mechanical response of the 3YSZ films [7]. Mechanical parameters such as hardness (H) and Young's modulus (E) were obtained from these tests [10,11]. The tests were performed at a load of 1.8 mN using a Berkovich indenter (three-sided pyramid).

3. Results and discussion

3.1. Microstructural evolution

Fig. 1 shows XRD patterns of 3YSZ films sintered in the range of temperatures between 280 °C and 500 °C. The diffractograms correspond to 2-layers 3YSZ films deposited on soda-lime glass substrates instead of on sapphire substrates because they were collected only to measure the crystallization temperature and the sapphire peak could complicate the observation of weak peaks from the 3YSZ films. From Fig. 1, it is deduced that the crystallization temperature in 3YSZ films is located at around 290–300 °C. At lower temperatures, the 3YSZ films are amorphous. From 300 °C, as the sintering

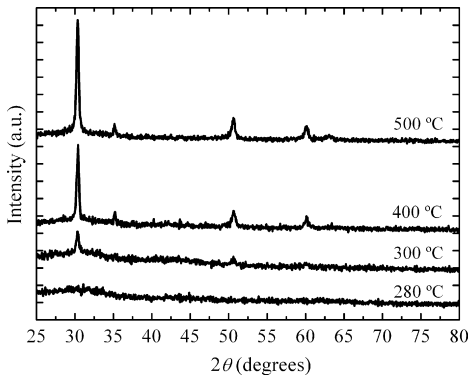

Fig. 1. Experimental XRD patterns of 3YSZ films on soda-lime glasses sintered in the range of temperatures between 250 °C and 500 °C.

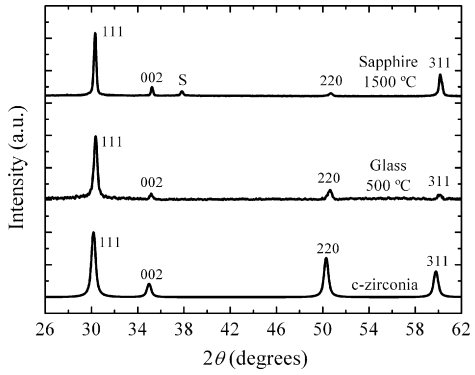

Fig. 2. Experimental XRD patterns of 3YSZ films after sintering at 500 °C and 1500 °C. The peak noted as S corresponds to the sapphire substrate. The theoretical zirconia cubic phase pattern has also been included for comparison.

temperature increases the 3YSZ films become more crystalline as shown by the increase in the intensity of the XRD peaks. In addition, it is also seen that the 3YSZ films crystallize in the cubic system.

Fig. 2 shows the XRD patterns obtained from 10-layers 3YSZ films and sintered in the range of temperatures between 500 °C and 1500 °C. As can be observed, the cubic phase is stable in the entire sintering interval, a fact that was further confirmed by the Rietveld analysis of the XRD patterns. The presence of the cubic phase was not an unexpected result despite previous reports in the literature suggest an exclusively tetragonal composition for these yttria contents (3 mol%) [17] or the coexistence of the tetragonal and cubic phases [18]. This assumption, acceptable for bulk samples, is too simple to predict the composition of phases in a zirconia thin film obtained by the sol–gel route, where numerous factors (especially the variation of pH in the solution, the grain size within the nanometre range, and the thickness of each layer) can affect the final structure [19,20].

Fig. 3 shows a SEM image sequence obtained from 10-layers 3YSZ films deposited on sapphire and sintered in the range of temperatures between 800 °C and 1500 °C. It is observed that the densification of the films progressively increases as sintering temperature does, the complete densification being reached at a temperature around 1100 °C. This behaviour is in good agreement with other results previously reported by the authors [15]. One appreciates the progressive increase of grain size in the 3YSZ films as the sintering temperature rises. According to what one observes in the

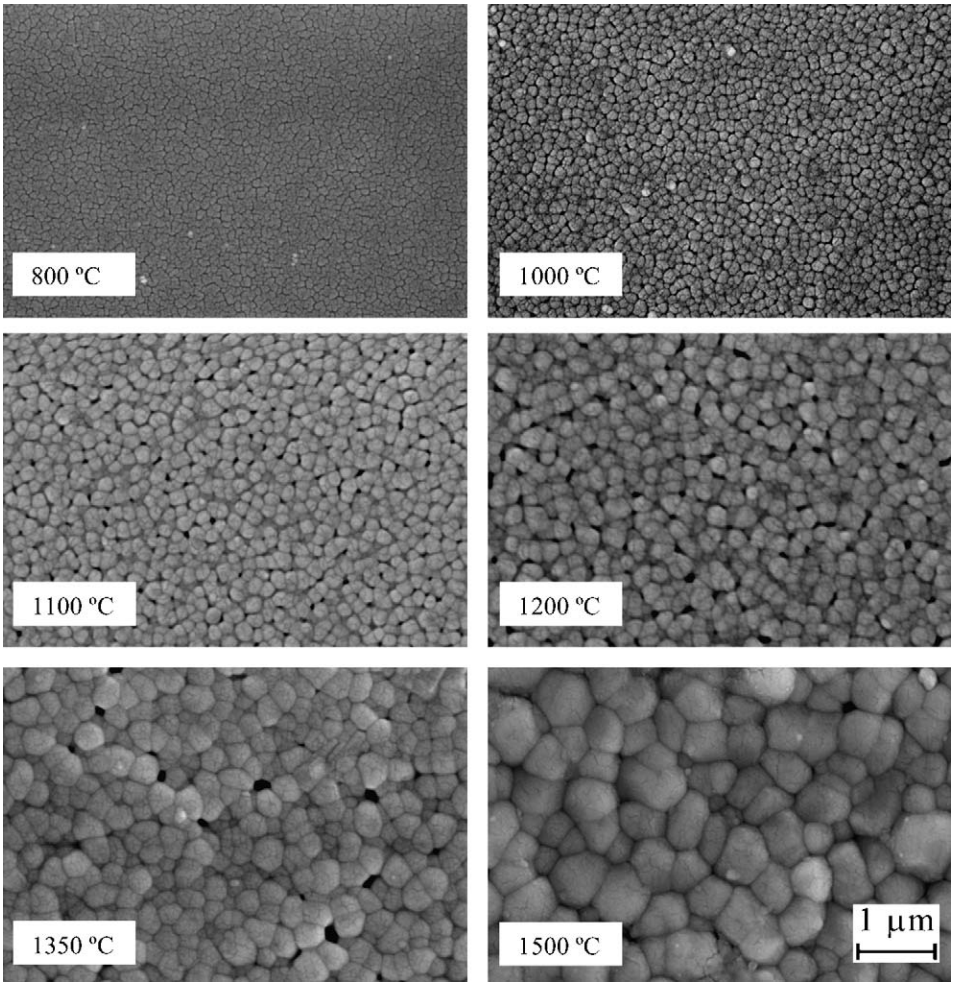

Fig. 3. SEM images of 3YSZ films sintered at temperatures between 800 °C and 1500 °C.

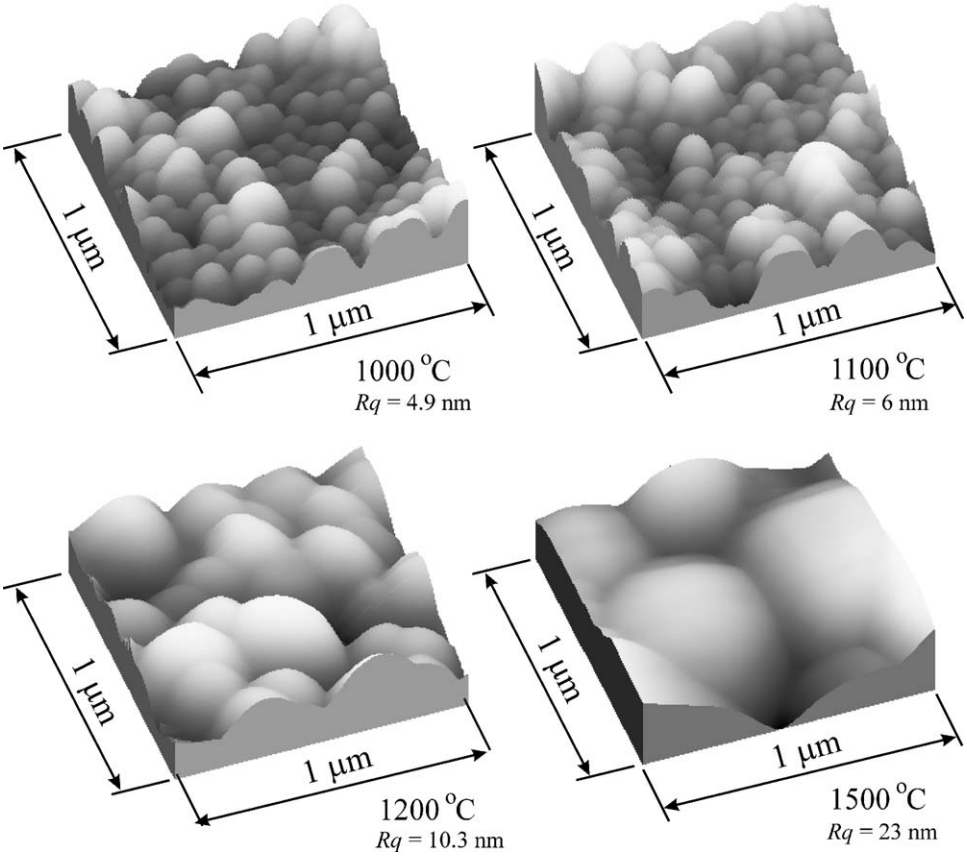

Fig. 4. AFM images of 3YSZ films sintered at temperatures between 1000 °C and 1500 °C. *Rq* correspond to the mean quadratic roughness of the coating.

images, this increase seems to be caused by the progressive agglomeration of smaller grains.

This same trend can be appreciated in Fig. 4, which shows the images obtained by AFM on 10-layers 3YSZ films sintered in the range of temperatures between 1000 °C and 1500 °C. A gradual increase of the grain size can be appreciated as the sintering temperature is increased, although this change is especially significant above 1100 °C. This increase is doubtless associated with diffusion phenomena favoured by the high sintering temperatures.

From the broadening of the Bragg reflection 1 1 1, the mean crystallite size was determined as a function of sintering temperature by the variance method. These values are shown in Fig. 5, together with roughness determined by AFM and the grain size determined by SEM. In Fig. 5, one observes the progressive increase of the grain (SEM) and crystallite (XRD) sizes as the sintering temperature increases especially above 1000 °C [21,22]. Nevertheless, the grain size presents a greater growth rate than the crystallite size, suggesting that the growth of the grains takes place at the expense of the clustering of the crystallites. This hypothesis is consistent with the SEM and AFM micrographs shown previously. Fig. 5 also shows that the roughness increases with increasing sintering temperature. This could be associated with the increase of the grain size, causing

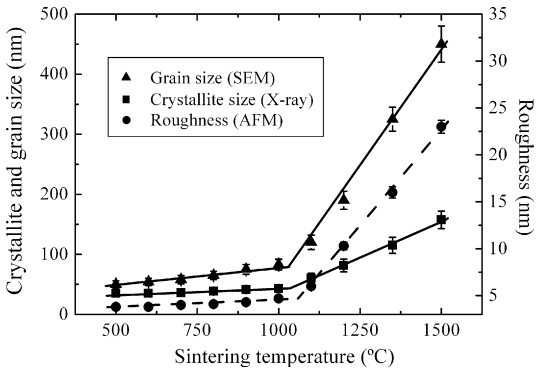

Fig. 5. Grain size, crystallite size, and roughness of the 3YSZ films sintered in the range of temperatures between 500 °C and 1500 °C.

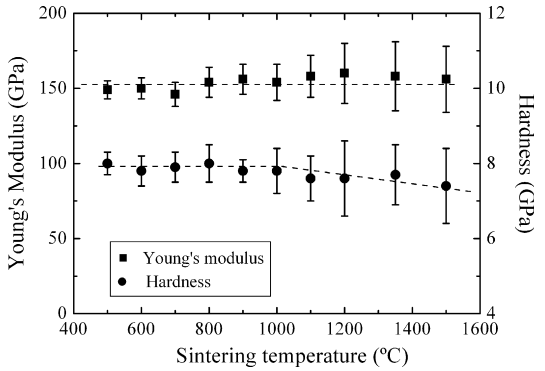

Fig. 6. Hardness and Young's modulus from nanoindentation tests in 3YSZ films sintered at temperatures between 500 °C and 1500 °C.

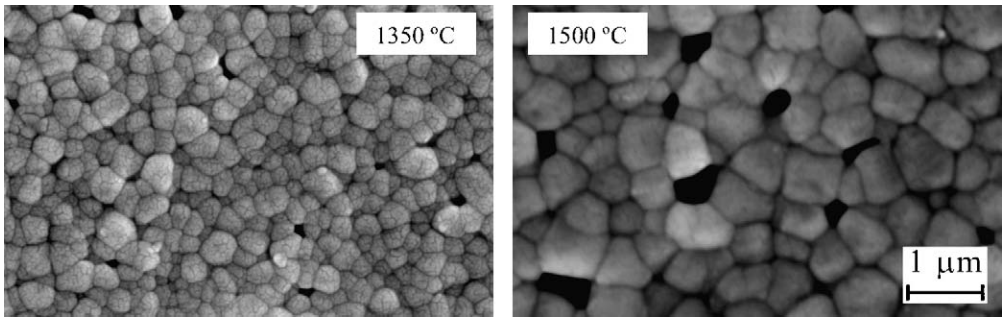

Fig. 7. SEM images of 3YSZ films sintered at temperatures above 1200 °C. The images show the formation of cavities in the films above 1300 °C.

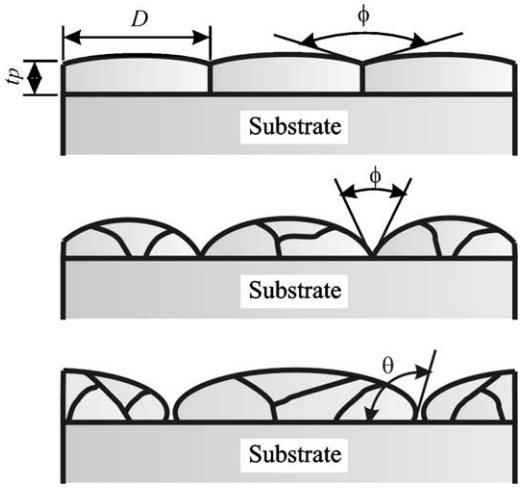

Fig. 8. Schematic representation of grain clustering phenomenon in zirconia thin films. The grain size, D, is greater than the thickness of the layer, t_p.

greater differences between the hills and valleys of the profile detected by AFM.

3.2. Mechanical characterization

Fig. 6 shows the hardness (H) and Young's modulus (E) of the 3YSZ films determined by nanoindentation tests. It can be concluded that Young's modulus (approximately 175 GPa) does not depend on the sintering temperature. This is not surprising because Young's modulus is a characteristic of the material and should present little fluctuation even varying considerably the percentage of Y_2O_3 (2–10%) with which the ZrO_2 is doped [23]. Nevertheless, one appreciates a slight decrease in the hardness values above sintering temperatures of 1000 °C, temperatures at which the complete densification of the 3YSZ films takes place [24]. This variation in the hardness values could be associated with the increased grain size observed at high temperatures [25], as is reflected in the SEM and AFM images and in the XRD analysis. Also, these values are in consonance with other hardness values reported in the literature for these materials in the form of thin films [26].

It is interesting to notice the large uncertainty (shown by larger error bars) in the values of H and E for high sintering temperatures (1350–1500 °C). This effect, as well as the increased roughness of the coatings shown in Figs. 4 and 5, could be associated with a phenomenon of deterioration of the layers observed at high sintering temperatures (see Fig. 7). In particular, the high sintering temperatures induce a process of grain spheroidization [27,28]. This phenomenon of grain clustering has been observed before in films of a similar composition to that used in this work whenever the grain size is greater than the thickness of the layer (see Fig. 8). In this situation, certain critical thermodynamic conditions and dewetting process can arise that favour this type of phenomenon [29,30]. These results suggest the interest of obtaining fully dense films to improve further the mechanical protection they offer to the substrates.

4. Concluding remarks

We have studied the microstructural evolution and mechanical behaviour of 3YSZ films sintered in air between 100 °C and 1500 °C. Crystallization occurs at around 290–300 °C, in the cubic system. The cubic phase of ZrO_2 remains stable up to temperatures of 1500 °C. There is a gradual increase in the grain and crystallite sizes in the film structure. This occurs from 500 °C until approximately 1000 °C. Above this sintering temperature, this tendency changes abruptly, with a rapid increase in grain and crystallite sizes until temperatures close to 1500 °C. This increase is associated with diffusion phenomena favoured by the high temperatures. With respect to the mechanical behaviour of the films, one can conclude that Young's modulus does not depend on the sintering temperature. Nevertheless, a slight decrease in the hardness values is appreciated above temperatures of 1000 °C, which is due to the increase of the crystallite and grain sizes, which pass from the nano- to the microdomain. Consequently, by selecting the suitable sintering temperature, it will be possible to obtain zirconia films with microstructure and mechanical properties optimized to satisfy the requirements of specific applications.

Acknowledgments

The authors thank Dr. F. Guiberteau and Dr. A. Pajares for assistance in nanoindentation experiments and the useful discussions. They also gratefully acknowledge Conicet (Argentina) and the Ministerio de Educación, Cultura y Deporte (Spain) under Grant SB2000-0087 for supporting the stay of Dr Caruso in Spain. This study was supported by

funds from Consejería de Educación, Ciencia y Tecnología, Junta de Extremadura (Spain)-Fondo Social Europeo under Grant PRI07A070.

References

[1] C.J. Brincker, G.W. Scherer, Sol–Gel Science: The Physics and Chemistry of Sol–Gel Processing, Academic Press, San Diego, 1990.
[2] R. Gvishi, Fast sol–gel technology: from fabrication to applications, J. Sol–gel Sci. Technol. 50 (2) (2009) 241–253.
[3] M. Ohring, The Materials Science of Thin Films, Academic Press, London, 1992.
[4] C. Viazzi, J.P. Bonino, F. Ansart, Synthesis by sol–gel route and characterization of yttria stabilized zirconia coatings for thermal barriers applications, Surf. Coat. Technol. 201 (7) (2006) 3889–3893.
[5] D.J. Green, R.H. Hannink, M.W. Swain, Transformation Toughening of Ceramics, CRC Press, Boca Raton, FL, 1989.
[6] W.M. Liu, Y.X. Chen, C.F. Ye, et al., Preparation and characterization of doped sol–gel zirconia films, Ceram. Int. 28 (4) (2002), 349-345.
[7] R. Caruso, A. Díaz-Parralejo, P. Miranda, et al., Controlled preparation and characterization of multilayer sol–gel zirconia dip-coatings, J. Mater. Res. 16 (8) (2001) 2391–2398.
[8] Y. Ohya, H. Ishikawa, T. Ban, Microstructure and stress-induced phase transformation of sol–gel derived zirconia thin films, J. Ceram. Soc. Jpn. 114 (1329) (2006) 411–414.
[9] D.E. Ruddell, B.R. Stoner, J.Y. Thompson, The effect of deposition parameters on the properties of yttria-stabilized zirconia thin films, Thin Solid Films 445 (1) (2003) 14–19.
[10] J.L. Loubet, J.M. Georges, G. Meille, Microindentation Techniques in Materials Science and Engineering, in: P.J. Blau, B.R. Lawn (Eds.), American Society for Testing Materials STP, vol. 889, 1989.
[11] W.C. Oliver, G.M. Pahrr, An improved technique for determining hardness and elastic-modulus using load and displacement sensing indentation experiments, J. Mater. Res. 7 (6) (1992) 1564–1583.
[12] L. Riester, M.K. Ferber, in: R.C. Bradt, C.A. Brookes, J.L. Routbort (Eds.), Plastic Deformation of Ceramics, Plenum Press, New York, 1995.
[13] B.J. Gomez, R. Caruso, L. Nachez, et al., Influence of ion nitriding process on the properties of zirconia coatings deposited on stainless steel, Braz. J. Phys. 36 (3B) (2006) 1000–1003.
[14] M. Guglielmi, S. Zenezini, The thickness of sol–gel silica coatings obtained by dipping, J. Non-Cryst. Solids 121 (1–3) (1990) 303–309.
[15] A. Díaz-Parralejo, R. Caruso, A.L. Ortiz, et al., Densification and porosity evaluation of ZrO_2-3 mol% Y_2O_3 sol–gel thin films, Thin Solid Films 458 (1–2) (2004) 92–97.
[16] J. Bergmann, R. Kleeberg, Fundamental parameters versus learnt profiles using the rietveld program BGMN, European power diffraction, Mater. Sci. Forum. 378 (3) (2004) 30–35.
[17] P.M. Kelly, L.R.F. Rose, The martensitic transformation in ceramics – its role in transformation toughening, Prog. Mater. Sci. 47 (5) (2002) 463–557.
[18] M.X. Zhang, P.M. Kelly, Crystallographic features of phase transformations in solids, Prog. Mater. Sci. 54 (8) (2009) 1101–1170.
[19] G.K. Chuah, S.H. Liu, S. Jaenicke, et al., High surface area zirconia by digestion of zirconium propoxide at different pH, Micropor. Mesopor. Mater. 39 (1–2) (2000) 381–392.
[20] A.L. Ortiz, A. Díaz-Parralejo, O. Borrero-Lopez, et al., Effect of ion nitriding on the crystal structure of 3 mol% Y_2O_3-doped ZrO_2 thin films prepared by the sol–gel method, Appl. Surf. Sci. 252 (17) (2006) 6018–6021.
[21] S.Y. Bae, H.S. Choi, S.Y. Choi, et al., Sol–gel processing for epitaxial growth of ZrO_2 thin films on Si(1 0 0) wafers, Ceram. Int. 26 (2) (2000) 213–214.
[22] I. Zlotnikov, I. Gotman, E.Y. Gutmanas, Characterization and nanoindentation testing of thin ZrO_2 films synthesized using layer-by-layer (LbL) deposited organic templates, Appl. Surf. Sci. 255 (5) (2008) 3447–3453.
[23] L. Kondoh, H. Shiota, K. Kawachi, et al., Yttria concentration dependence of tensile strength in yttria stabilized zirconia, J. Alloy Compd. 365 (1–2) (2004) 253–258.
[24] M.J. Paterson, P.J.K. Paterson, B. Ben-Nissan, The dependence of structural and mechanical properties on film thickness in sol–gel zirconia films, J. Mater. Res. 13 (2) (1998) 388–395.
[25] S. Martorana, A. Fedele, M. Mazzocchi, et al., Surface coatings of bioactive glasses on high strength ceramic composites, Appl. Surf. Sci. 255 (13–14) (2009) 6679–6685.
[26] H.L. Wang, M.J. Chiang, M.H. Hon, Determination of thin films hardness for a film/substrate system, Ceram. Int. 27 (4) (2001) 385–389.
[27] R. Guinebretiere, B. Soulestin, A. Dauger, XRD and TEM study of heteroepitaxial growth of zirconia on magnesia single crystal, Thin Solid Films 319 (1–2) (1998) 197–201.
[28] A. Boulle, R. Guinebretiere, O. Masson, et al., Recent advances in high-resolution X-ray diffractometry applied to nanostructured oxide thin films: the case of yttria stabilized zirconia epitaxially grown on sapphire, Appl. Surf. Sci. 253 (1) (2006) 95–105.
[29] K.T. Miller, F.F. Lange, D.B. Marshall, The instability of polycrystalline thin-films – experiment and theory, J. Mater. Res. 5 (1) (1996) 151–160.
[30] A. Boulle, L. Pradier, O. Masson, et al., Microstructural analysis in epitaxial zirconia layers, Appl. Surf. Sci. 188 (1–2) (2002) 80–84.